Food Chemistry: X 25 (2025) 102095

Contents lists available at ScienceDirect

Food Chemistry: X

journal homepage: www.sciencedirect.com/journal/food-chemistry-x

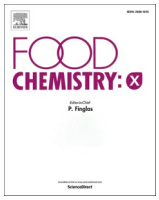

The mitochondrial functional characteristics and microstructure play an important role in yak meat color during wet curing

Zhuo Wang [a], Jibing Ma [b], Guoyuan Ma [a,*], Qunli Yu [a,*], Ling Han [a], Li Zhang [a]

[a] College of Food Science and Engineering, Gansu Agricultural University, Lanzhou 730070, China
[b] Academy of Animal Science and Veterinary Medicine, Qinghai University, Xining 810016, China

ARTICLE INFO

Keywords:
Low-dose sodium nitrite
Yak meat color
Mitochondrial function and structure
Lipid oxidation products
OPLS-DA

ABSTRACT

The study investigated the impact of low-dose sodium nitrite on yak meat color and mitochondrial functional characteristics during the wet curing. The results showed that sodium nitrite significantly enhanced the redness (a^* value) of yak meat by increasing the activities of mitochondrial complexes I, II, III and IV, which are critical for electron transport and aerobic respiration. Additionally, sodium nitrite reduced mitochondrial swelling and membrane permeability, and slowed the production of lipid oxidation products, indicating protective effects against mitochondrial damage and preserving mitochondrial integrity. Correlation analysis and Orthogonal Partial Least Squares Discriminant Analysis (OPLS-DA) identified mitochondrial complex I activity, NADH-dependent metmyoglobin reductase activity, and specific lipid oxidation products as key factors influencing the a^* value of yak meat. These findings highlighted the significant role of mitochondrial function and structure in meat color stability.

1. Introduction

Meat color is one of the most important quality attributes of meat products and serves as a crucial indicator for consumers to judge the quality of the meat, directly influencing their purchasing decisions (Li et al., 2017). The mechanisms behind the color changes in postmortem muscle and the methods to preserve meat color have been central topics in the field of meat science. After animal bleeding, the color of the meat is primarily determined by the content and chemical state of myoglobin (Ma et al., 2022). Myoglobin is a globular heme protein composed of globin and heme (Alazoumi et al., 2021). The state of the iron atom in the heme and the type of ligand bound to it determine the form of myoglobin, thus giving rise to different meat colors (Suman & Joseph, 2013). Typically, when the iron atom in the heme is in the Fe^{2+} state and the sixth coordination site is not bound to a ligand, the myoglobin is in the deoxymyoglobin form, which gives the meat a dark red color; If the sixth coordination site is bound to oxygen, the myoglobin becomes oxymyoglobin, imparting a cherry-red color to the meat, which is preferred by consumers (Mancini & Hunt, 2005). However, the Fe^{2+} state in heme is highly unstable and easily oxidizes to the more stable Fe^{3+} state, converting myoglobin to metmyoglobin, which causes the meat to turn a brown color that is generally unacceptable to consumers (Attri et al., 2014).

Mitochondria, composed of a double membrane structure formed by a phospholipid bilayer, are the primary sites for aerobic respiration and electron transport in the body, and are responsible for the majority of the body's energy production (Zhang et al., 2019). In the early postmortem period, mitochondria in muscle cells can still perform aerobic respiration and electron transport. This is because, after bleeding, the cells' pathway to obtain oxygen from the blood is cut off, with myoglobin serving as a temporary oxygen reservoir in the body (Tang, Faustman, Hoagland, et al., 2005). At this time, myoglobin becomes the main source of oxygen for muscle cells, delivering oxygen to the mitochondria for aerobic respiration. The loss of oxygen from myoglobin converts it to a deoxy state, which darkens the color of the meat (Kuleva et al., 2016). Therefore, mitochondria are closely related to the redox state of myoglobin and the stability of meat color. Mitochondria influence the redox state of myoglobin through two main mechanisms: oxygen consumption and the reduction of metmyoglobin (Gao et al., 2013). On one hand, increased oxygen consumption promotes the conversion of oxymyoglobin to deoxymyoglobin, which is more easily oxidized to metmyoglobin, leading to meat browning (Gao et al., 2013). On the other hand, electrons from the mitochondrial electron transport chain can directly reduce metmyoglobin (Tang, Faustman, Mancini, et al., 2005).

* Corresponding authors.
E-mail addresses: maguoyuangsau@163.com (G. Ma), yunqunligau@163.com (Q. Yu).

https://doi.org/10.1016/j.fochx.2024.102095
Received 5 October 2024; Received in revised form 24 November 2024; Accepted 11 December 2024
Available online 20 December 2024

Studies have shown that factors affecting mitochondrial structure and function, such as pH, aging time, and lipid oxidation, also impact meat color (Faustman et al., 2010; Gagaoua et al., 2015; Mancini & Ramanathan, 2014). There is scarce information regarding the relationship between changes in mitochondrial functional characteristics and microstructure and meat color stability.

Sodium nitrite is a unique additive used in meat products. High concentrations of sodium nitrite can react with DNA, leading to mutations and posing potential health risks to humans (Bedale et al., 2016). However, in recent years, the positive effects of using low concentrations of sodium nitrite have gained increasing attention. On one hand, sodium nitrite can inhibit microbial growth, significantly reducing the production of botulinum toxin and delaying spoilage during storage (Sallan et al., 2020). On the other hand, sodium nitrite applied to meat products can mitigate the autoxidation of muscle myoglobin as well as the lipid and protein oxidation catalyzed by autoxidation (Ma et al., 2021). In this process, $NaNO_2$ acts as a reducing agent, converting the oxidized high-valence state of myoglobin heme iron back to its native state. This not only alters the physicochemical properties of myoglobin but, more importantly, reduces the formation of harmful substances in meat caused by oxidation (Sullivan & Sebranek, 2012). Low-dose sodium nitrite refers to the addition of less than 60 mg/kg sodium nitrite during processing (Lee et al., 2018). Our previous study demonstrated the protective characterization of low-dose sodium sodium nitrite on yak meat myoglobin (Ma et al., 2019). Given the close relationship between the redox state of myoglobin and mitochondria, further research is needed to explore the impact of sodium nitrite on mitochondrial function and structure and its relationship with meat color. This study provides insight regarding the roles of coordinated regulation of $NaNO_2$ and mitochondria in development of color stability of yak meat.

2. Materials and methods

2.1. Meat samples

Six healthy yaks, aged 3 to 4 years and with an average body weight of 250 kg, were selected from the same pasture under identical natural grazing conditions and fed a uniform diet from the same batch of feed. These yaks were humanely slaughtered at a commercial meat processing facility (Qinghai Baide Food Co. Ltd., Qinghai, China). This procedure was conducted according to the "Operating Procedures of Cattle Slaughter" of the National Standards of PR China including animal welfare and conditions. After slaughter, *longissimus thoracic* muscles were removed from the carcasses immediately and cut into 10 × 5 × 2 cm^3 cubes. The samples were randomly divided into two groups. One group was injected with 90 mg/L sodium nitrite solution, and the injection method was performed based on our previous report (Ma et al., 2021). Another group was injected with distilled water in the same ratio. All samples were stored at 4 °C for curing, and collected form the refrigerator at the end of day 0 (no injection), 1, 3, 5 and 7 for biochemical analysis.

2.2. Measurement of redness values (a*)

The values of muscle redness (a^*) were measured by a CR410 colorimeter (Ma et al., 2022). After preheating the colorimeter for 30 min, calibrate it using a white board. For each group of samples, expose fresh cuts (thickness over 1 cm) to air for 30 min before selecting three different areas for measurement.

2.3. Determination of mitochondrial complex activities

Activities of mitochondrial complexes I, II, III, IV and V were determined by Micro Mitochondrial Respiratory Chain Complex I (BC0515), II (BC3235), III (BC3240), IV (BC0945) and V (BC1445) Activity Assay Kits (Solarbio, Beijing, China) following the instructions of the manufacturer, respectively. Weigh 1 g of the muscle sample, add the reagents sequentially according to the kit instructions, and then proceed with the analysis.

2.4. Activity analysis of Na^+/K^+-ATPase

Na^+/K^+-ATPase activity was determined spectrophotometrically using a Micro Na^+/K^+-ATPase Activity Assay Kit (BC0065, Solarbio, Beijing, China) following the instructions of the manufacturer.

2.5. NADH-dependent metmyoglobin reductase activity assay

The assay was conducted according to Elroy et al. (2015) and Reddy, and M., and Carpenter, C. E. (1991) with minor modifications. Briefly, muscle samples (10 g) were homogenized in 1 mL of 2.0 mM phosphate buffer solution (pH 7.0). The homogenate was then centrifuged at 8000*g* for 20 min. The supernatant was filtered using filter paper, and potassium ferrocyanide was added to the filtrate. The filtrate was dialyzed at 4 °C for 24 h. The phosphate buffer was needed to be replaced 5 times to remove excess potassium ferrocyanide. The dialysate was then centrifuged at 8000*g* for 20 min. The supernatant was diluted with phosphate buffer solution to 20 mL and used as crude enzyme extracts. Subsequently, 0.6 mL of crude enzyme extracts was incubated with 0.1 mL 5 mM EDTA, 0.1 mL 5 mM Tris-HCl, 0.1 mL 3 mM $K_4Fe(CN)_6$, 0.1 mL deionized water and 0.2 mL 0.75 mM metmyoglobin standard solution for 30 min at 25 °C. Then, 0.2 mL of 2 mM NADH was added and the absorbance value at 580 nm was immediately measured as A_1. After 1 min of reaction, the absorbance value was determined to be A_2. The NADH-dependent metmyoglobin reductase activity was calculated according to the formula:

$$\mathrm{U\ (nmol/(}\textit{ming}\ \mathrm{meat))} = (A_2 - A_1)/\mathrm{T}^*(\mathrm{V}^*10^{-}9)/(\varepsilon^*\mathrm{v}^*\mathrm{d}^*\mathrm{m})$$

in which, T is the reaction time of 1 min, V is the total volume of the reaction (mL), ε is the molar extinction coefficient of 12,000, v is the sample volume (0.6 mL), d is the optical path of 1 cm, and m is the muscle sample weight of 10 g.

2.6. Isolation of mitochondria

Muscle mitochondria were isolated as previously reported (Zhang et al., 2017). Briefly, 10 g fresh muscle samples were homogenized in 90 mL of isolation buffer containing 0.25 M sucrose, 20 mM HEPES, 10 mM Tris-HCl, 1 mM EDTA, 0.5 % bovine serum albumin (pH 7.4). The homogenate was centrifuged for 15 min at 1000*g*. The supernatant was then centrifuged for 15 min at 1000*g*, and the obtained supernatant was centrifuged again for 20 min at 12,000*g*. The pellet was finally suspended in suspension buffer (0.25 M sucrose, 20 mM HEPES, 10 mM Tris-HCl, 1 mM EDTA, pH 7.4).

2.7. Mitochondrial swelling and membrane permeability

The mitochondrial pellet (0.5 mg/mL, 3 mL) was incubated with 0.4 mL of 0.5 mM $FeSO_4$ and 0.4 mL of 0.5 mM ascorbic acid for 15 min at 37 °C. The mitochondrial swelling was analyzed by determining the light absorption value at 520 nm (Zhang et al., 2019).

The evaluation of mitochondrial membrane permeability was performed according to Wang et al. (2018). Briefly, 300 μL of mitochondrial pellet (3 g/L) was incubated with 2700 μL of test medium (230 mM mannitol, 70 mM sucrose, 3 mM HEPES, pH 7.4) for 3 min at 25 °C. The absorbance value was measured at 540 nm (UV2550 spectrophotometer, Shimadzu, Japan).

2.8. Transmission electron microscopy

The method was conducted according to Rybka et al. (2019) with

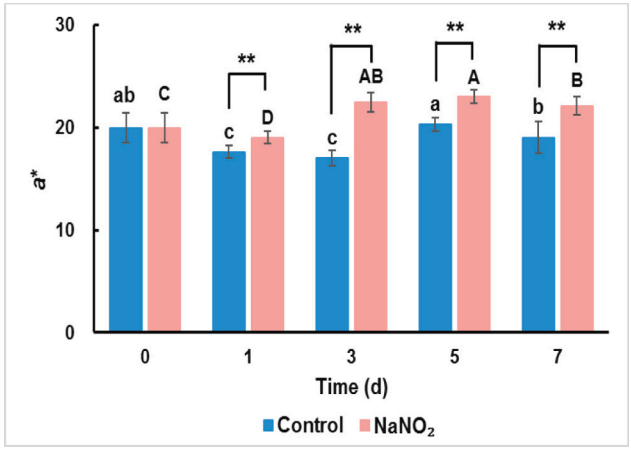

(A)

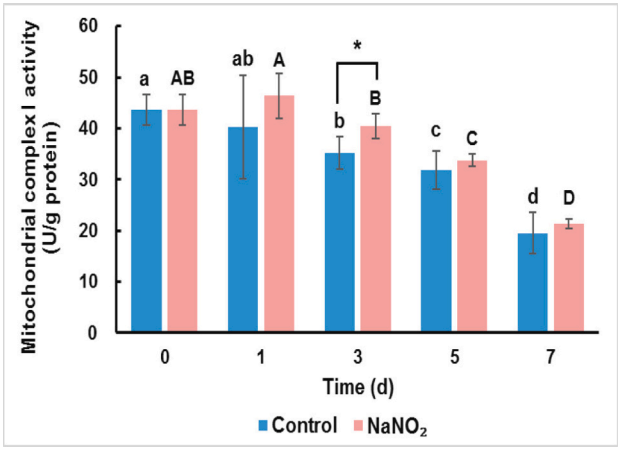

(B)

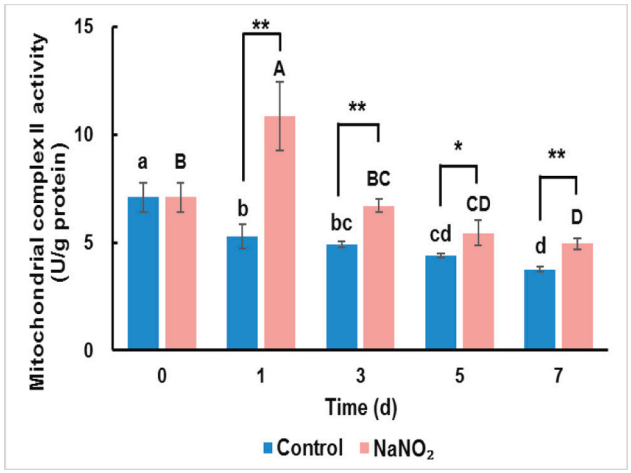

(C)

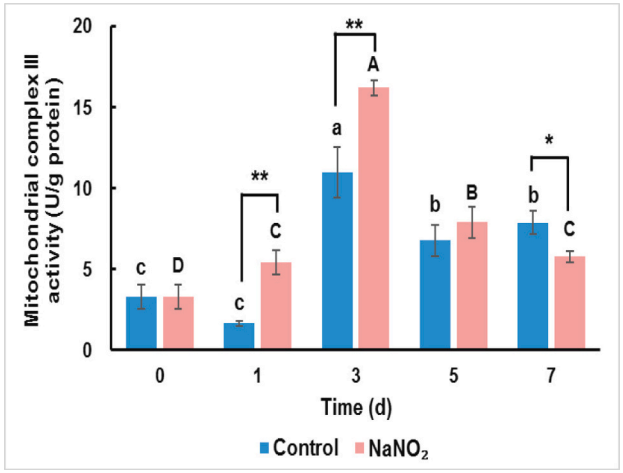

(D)

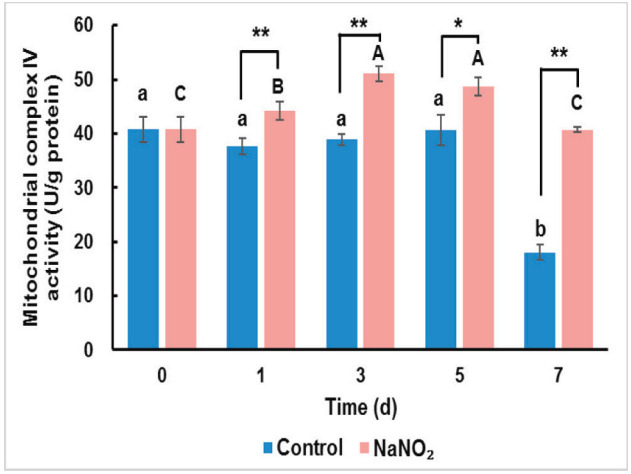

(E)

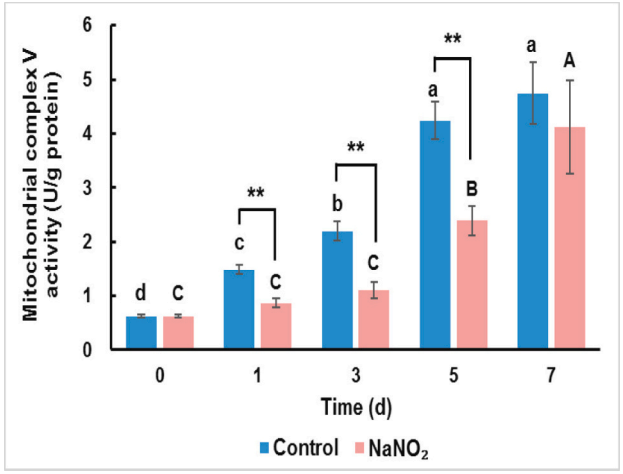

(F)

Fig. 1. Effect of low-dose nitrite on the meat color and mitochondrial related enzyme activities. (A) a^* value. (B) Mitochondrial complex I activity. (C) Mitochondrial complex II activity. (D) Mitochondrial complex III activity. (E) Mitochondrial complex IV activity. (F) Mitochondrial complex V activity. (G) Na^+/K^+-ATPase activity. (H) NADH-dependent MMb reductase activity. The small letters and capital letters in the figure respectively indicate the significant difference between the control group and the $NaNO_2$ group ($P < 0.05$). The * indicates the significant difference between groups, *: ($P < 0.05$); **: ($P < 0.01$).

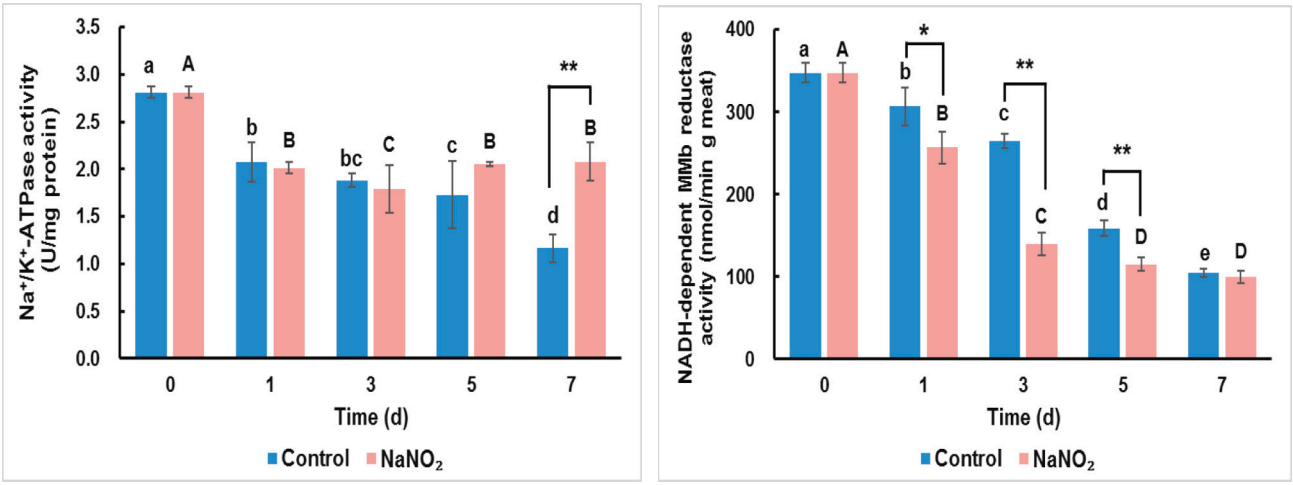

(G) (H)

Fig. 1. (*continued*).

minor modifications. The meat samples were cut into 1 × 3 × 3 mm^3 pieces and soaked in 2.5 % glutaraldehyde for 4 h. The pieces were washed with 0.1 M phosphate buffer solution (pH 7.4), and then soaked in 1 % osmic acid for 2 h. After dehydration, the pieces were embedded in the solution (acetone: resin = 2:1, *w*/w) for 12 h at 40 °C. The embedded samples were then dried at 60 °C for 15 min. Subsequently, the samples were aggregated, sliced, stained, and transferred into the TEM (H7500, HITACHI, Japan). The generated images were recorded electronically.

2.9. Mitochondrial lipid oxidation products

2.9.1. Sample preparation

The types and contents of volatile compounds were determined using SPME-GC–MS technology (Bueno et al., 2019). 1 mL of mitochondrial solution (1 mg/mL), 0.4 g of sodium chloride, and 20 μL of 0.06 μg/L BHT (Butylated Hydroxytoluene) as an internal standard were taken and placed in a headspace extraction vial equipped with a silicone septum, and then mixed thoroughly. The headspace vial was shaken at a constant temperature of 90 °C for 5 min and then subjected to headspace extraction for 15 min using an SPME extraction head. After extraction, the compounds were desorbed for 5 min at the GC–MS injection port at 250 °C.

2.9.2. GC–MS conditions

Chromatographic conditions: The chromatographic column used was a Thermo TG-WAX (60 m × 0.25 mm, 0.5 μm). The temperature program was as follows: the initial column temperature was 35 °C, maintained for 5 min, then increased to 250 °C at a rate of 5 °C/min, and maintained for 5 min. The carrier gas (He) flow rate was 0.8 mL/min, with no split.

Mass spectrometry conditions: Electron impact (EI) ion source had an electron energy of 70 eV, an ion source temperature of 230 °C, a transfer line temperature of 250 °C, and a quadrupole temperature of 150 °C. The mass scan range was *m/z* 40–600, in full scan mode.

2.9.3. Qualitative and quantitative analysis of volatile compounds

Qualitative analysis: Qualitative analysis was performed by comparing the obtained spectra with the NIST 14 library.

Quantitative analysis: Qualitative was done using the internal standard method. The concentration of volatile substances (mg/kg) was calculated using the formula:

$$C\ (\mathrm{mg/kg}) = (Cs \times Vs \times Ae)/(As \times M)$$

where *C* is the content of volatile substances (mg/kg), *Cs* is the internal standard concentration (μg/L), Vs is the internal standard volume (μL), *Ae* is the peak area of each component, *As* is the peak area of the internal standard, *M* is the mitochondrial mass (kg).

2.10. Statistical analysis

The data from different curing times (0, 1, 3, 5, and 7 d) were analyzed by using Analysis of Variance Procedure. The differences between the mean values were compared by Duncan's multiple range test ($P < 0.05$). The Student *t*-test was used to compare the two different groups ($^*P < 0.05$, $^{**}P < 0.01$). Each assay was performed in triplicate. Perform orthogonal partial least squares discriminant analysis (OPLS-DA) using SIMCA 14.1 software.

3. Results and discussion

3.1. Meat color and mitochondrial related enzyme activities

The effect of low-dose sodium nitrite on the meat color of yak is depicted in Fig. 1A. The a^* value in the both control and $NaNO_2$ group decreased and the increased during the wet curing ($P < 0.05$), which is related to the state of myoglobin. After yak slaughter and bleeding, the oxygen supply to the muscles becomes insufficient. Myoglobin delivers oxygen to the mitochondria and is itself deoxygenated, converting into deoxymyoglobin. When oxygen from the air gradually permeates into the muscle, the deoxymyoglobin acquires oxygen and is reconverted into oxymyoglobin (Kuleva et al., 2016). The $NaNO_2$ group exhibited much higher a^* value than that of the control group on days 1, 3, 5 and 7 curing ($P < 0.01$), thereby indicating that the use of sodium nitrite resulted in the brighter red meat color of yak meat. During the curing of meat products, sodium nitrite reacts with myoglobin in the meat to form nitrosomyoglobin (MbNO), which gives the meat a tempting cherry red color (Gupta et al., 2018).

The mitochondrial electron transport chain is closely related to the redox state of myoglobin, which determines meat color (Gao et al., 2013). The electron transport chain is a crucial pathway for the mitochondria-mediated reduction of metmyoglobin (Zou, Jia, et al., 2023). The components involved primarily include flavoproteins, iron-sulfur proteins, cytochromes, and ubiquinone, which form

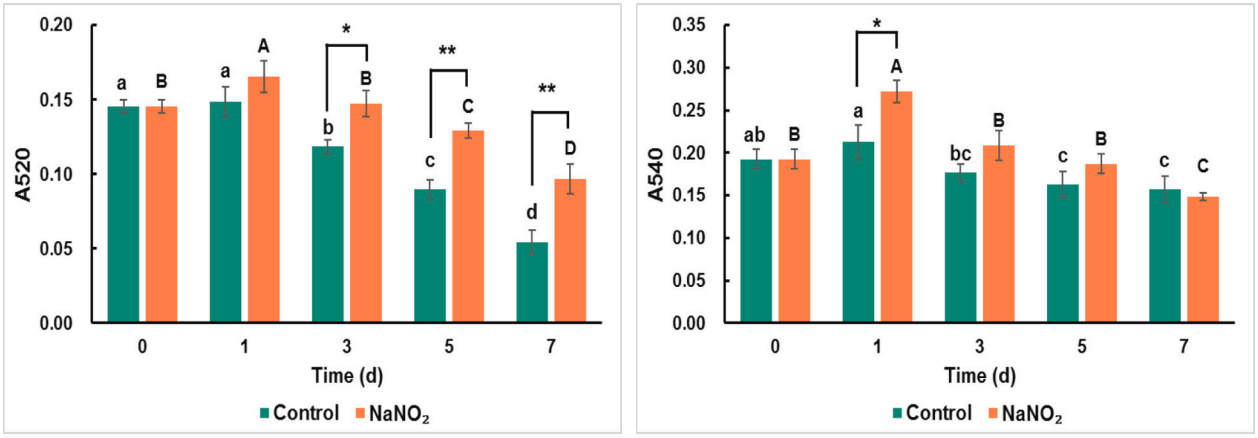

(A) (B)

Fig. 2. Effect of low-dose nitrite on (A) mitochondrial swelling and (B) mitochondrial membrane permeability. The small letters and capital letters in the figure respectively indicate the significant difference between the control group and the $NaNO_2$ group ($P < 0.05$). The * indicates the significant difference between groups, *: ($P < 0.05$); **: ($P < 0.01$).

complexes on the mitochondrial membrane surface: NADH-Q reductase (complex I), succinate-Q reductase (complex II), cytochrome reductase (complex III), and cytochrome oxidase (complex IV) (Zhao et al., 2019). Therefore, the effect of low-dose sodium nitrite on the mitochondrial complexes activities of yak was studied. As shown in Fig. 1(B—F), the mitochondrial complex I activity in the both control and $NaNO_2$ group decreased during the wet curing ($P < 0.05$). The activities of mitochondrial complex II, III and IV in the $NaNO_2$ group increased and then decreased during the wet curing ($P < 0.05$). The mitochondrial complex V activity in the both control and $NaNO_2$ group increased during the wet curing ($P < 0.05$). Most notably, the $NaNO_2$ group showed the higher activities of mitochondrial complex I, II, III and IV than that of the control group, indicating that low-dose sodium nitrite enhances mitochondrial complexes (I, II, III and IV) activities during the wet curing. It is widely accepted that in the oxidative respiratory chain, complexes I and II in the mitochondrial membrane receive NADH and succinate, respectively, and transfer the detached H^+ to coenzyme Q. The latter releases H^+ into the medium and transfers electrons via complex III, cytochrome *c*, and complex IV to metmyoglobin, thereby reducing it (Genova & Lenaz, 2013). When the activity of mitochondrial complexes and respiration are inhibited, the reduction rate of metmyoglobin significantly decreases (Ramanathan et al., 2013; Tang, Faustman, Mancini, et al., 2005). The results of this study suggested that low-dose sodium nitrite enhances the activity of mitochondrial electron respiratory chain complexes, facilitating electron transport and aerobic respiration in mitochondria, which positively contributes to maintaining the bright red color of yak meat. In contrast, this study observed that the mitochondrial complex V activity in the $NaNO_2$ group was lower than that of the control group during the wet curing ($P < 0.01$). In intact mitochondria, complexes I and II embedded in the inner membrane obtain electrons from NADH and $FADH_2$, respectively, and transfer them downstream in the respiratory chain to react with oxygen associated with complex IV. Protons are pumped by the complexes from the matrix into the intermembrane space, forming an electrochemical gradient. This gradient drives protons back into the matrix through ATP synthase (complex V), which synthesizes ATP (Genova & Lenaz, 2013). ATP is an essential energy molecule within cells, and its synthesis premarily relies on bio-oxidation reactions (Boyman et al., 2020). Therefore, it can be seen that low-dose sodium nitrite inhibits ATP synthesis, which may be related to the antioxidant effects of sodium nitrite. The specific mechanisms require further investigation. Na^+/K^+-ATPase is a member of the P-type ATPase family, which transforms the energy of ATP to the transmembrane Na/K gradient that is used to create mitochondrial membrane potential and transport substances (Chkadua et al., 2022). As shown in Fig. 1G, the Na^+/K^+-ATPase activity in the $NaNO_2$ group decreased and then increased during the wet curing ($P < 0.05$). Importantly, the $NaNO_2$ group showed the higher Na^+/K^+-ATPase activity than that of the control group on day 7 curing ($P < 0.01$). These results revealed that the rate of ATP consumption increases with the extension of curing time, and the low-dose sodium nitrite enhances the rate of ATP consumption, which was also supported by the results of the mitochondrial complex V activity.

In recent years, the research on the action of NADH-dependent metmyoglobin reductase has been more in-depth, and its mechanism is relatively well understood. This reduction system primarily consists of cytochrome *b*5 reductase, cytochrome *b*5, and NADH in the mitochondrial membrane. NADH, serving as an electron donor, transfers electrons to cytochrome *b*5 reductase, which then transfers the electrons to cytochrome *b*5. The reduced cytochrome *b*5 subsequently transfers the electrons to the heme group of metmyoglobin, thereby reducing the ferric iron (Fe^{3+}) to ferrous iron (Fe^{2+}) (Belskie et al., 2015). In this study, the effect of low-dose sodium nitrite on the NADH-dependent metmyoglobin reductase activity of yak was investigated (Fig. 1H). The NADH-dependent metmyoglobin reductase activity in the both control and $NaNO_2$ group decreased during the wet curing ($P < 0.05$). Besides, the $NaNO_2$ group exhibited much lower NADH-dependent metmyoglobin reductase than that of the control group on days 1, 3 and 5 curing. NADH, as a coenzyme and hydrogen donor in the enzymatic reduction process of metmyoglobin, has a significant impact on meat color stability. Washington et al. (2008) reported that during the metmyoglobin reduction process, NADH is continuously consumed, which may affect the reduction efficiency of metmyoglobin. Gao et al. (2014) studied the effect of different NADH concentrations on metmyoglobin reduction capability and indicated that NADH promotes metmyoglobin reduction, with higher NADH concentrations accelerating the enzymatic reduction process of metmyoglobin. Therefore, the consumption of NADH during curing reduces NADH-dependent metmyoglobin reductase activity. Nevertheless, Bekhit et al. (2001) observed that NADH-dependent metmyoglobin reductase was not related to meat color. Therefore, the role of mitochondrial NADH-dependent metmyoglobin reductase in catalyzing metmyoglobin reduction remains controversial. Further research is needed on the effect of low-dose sodium nitrite on the NADH consumption.

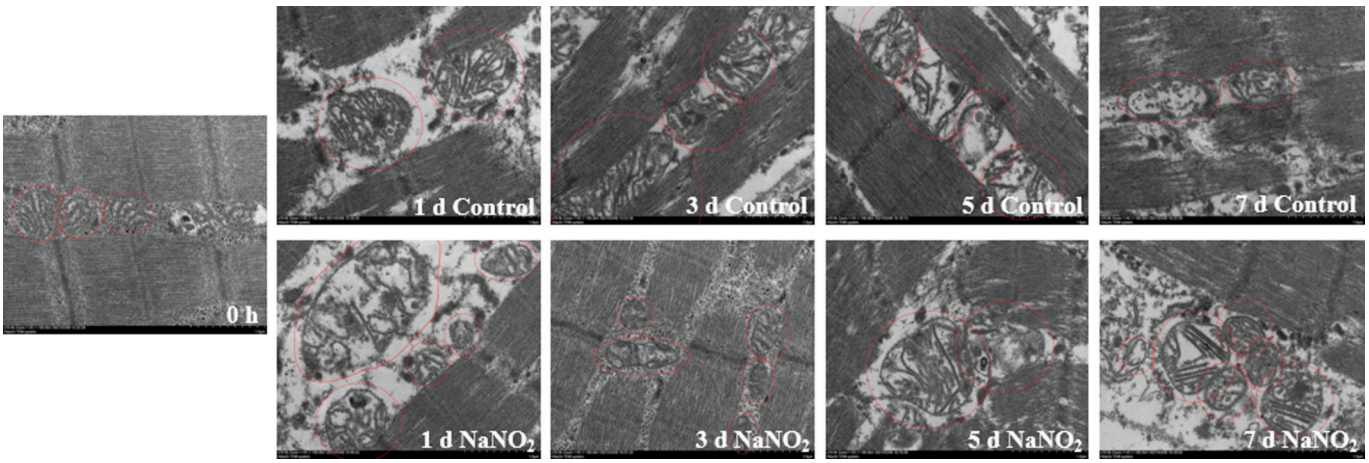

Fig. 3. Effect of low-dose nitrite on mitochondrial microstructure.

3.2. Changes in mitochondrial swelling and membrane permeability

The effect of low-dose sodium nitrite on the mitochondrial swelling and mitochondrial membrane permeability of yak is shown in Fig. 2. The lower the absorbance value is, the more light passing through the mitochondria, representing the greater mitochondrial swelling and membrane permeability (Zhang et al., 2019). As shown in Fig. 2, the mitochondrial swelling and membrane permeability in the both control and $NaNO_2$ group increased during the wet curing ($P < 0.05$). Besides, the control group exhibited much higher mitochondrial swelling than that of the $NaNO_2$ group on days 3, 5 and 7 curing, and showed much higher mitochondrial membrane permeability than that of the $NaNO_2$ group on day 1 curing. These results indicated that the mitochondrial membrane was damaged during the wet curing, however, low-dose sodium nitrite could protect mitochondrial membrane from damage.

Mitochondria are essential organelles in muscle cells responsible for storing and supplying energy to the body (Ramanathan et al., 2013). However, mitochondria are extremely sensitive to various types of damage, especially under conditions of energy substrate deprivation and low oxygen stress post-slaughter, which can easily damage their structure, impair their function, and eventually lead to cell death (Angelo et al., 2012). Mitochondrial damage primarily manifests in both structural and physiological functions (Mancini & Ramanathan, 2014). Specifically, structural damage includes increased membrane permeability, abnormal mitochondrial morphology and size, and a reduction in the number of mitochondria. The resulting physiological damage is characterized by the loss of marker enzyme activity, decreased concentrations of metabolic products, and reduced oxygen consumption rates (Gao et al., 2013). Mitochondrial membrane swelling and changes in membrane permeability are markers of structural damage, leading to changes in membrane fluidity, transmembrane potential, and membrane protein conformation. Damage to the mitochondrial membrane inevitably results in a decline in mitochondrial physiological function (Griffiths, 2000). Tang, Faustman, Hoagland, et al. (2005) observed that prolonged storage time causes mitochondrial structural swelling and destruction, thereby reducing mitochondrial viability. Chen et al. (2018) found that during storage, the permeability of beef mitochondrial membranes gradually increases, accompanied by a decrease in the activity of the mitochondrial energy metabolism marker enzyme SDH and MRA. In this study, mitochondrial membrane damage and a decline in NADH-dependent metmyoglobin reductase activity were observed during wet curing, suggesting that mitochondrial damage directly impairs the metmyoglobin reduction capacity. Therefore, the weakened activity of metmyoglobin reductase signifies that mitochondrial membrane damage leads to a decline in physiological function.

The present study also found that low-dose sodium nitrite could protect mitochondrial membrane from damage, which is closely related to the antioxidant properties of sodium nitrite. Numerous studies have demonstrated that mitochondrial swelling and membrane permeability elevated with the rise in reactive oxygen species (ROS) content (Wang et al., 2018; Zhang et al., 2020). Postmortem storage is a process of oxidative stress that inevitably generates ROS (Zhang et al., 2019). Sodium nitrite can inhibit the production of ROS by mitochondria (Raat et al., 2009). Furthermore, our previous study revealed that low-dose sodium nitrite enhanced the antioxidant capacity of muscle during the wet curing by improving the activity of some antioxidant enzymes and reducing the level of free radicals (Ma et al., 2021). Additionally, when the oxygen supply is reduced, deoxygenated myoglobin can catalyze the reduction of sodium nitrite to NO (Li et al., 2004), which is also confirmed by our previous report (Ma et al., 2021). At physiological levels, NO can act as an antioxidant interacting with hydrogen peroxide and superoxide (Wink et al., 2001). Furthermore, NO is known to reversibly bind to cytochrome *c* oxidase in complex IV. The release of cytochrome *c* oxidase is closely related to the mitochondrial membrane permeability (Tuell et al., 2021). NO can regulate release of cytochrome *c* by reducing the mitochondrial membrane permeability. In fact, it has been determined that NO actually prevents cytochrome *c* release (Kamga et al., 2012), indicating the role of low-dose sodium nitrite in regulating the mitochondrial membrane damage.

3.3. Changes in mitochondrial microstructure

To visually illustrate the extent of mitochondrial damage in yak meat during the wet curing, the changes in mitochondrial microstructure were studied from a morphological perspective. As shown in Fig. 3, the mitochondria in both the control and $NaNO_2$ groups gradually degraded with the extension of curing time. Specifically, on day 0 of curing, the mitochondria had a normal morphology, with a clear network structure and distinct inner and outer membranes. On day 1 of curing, the outer membranes of some mitochondria became blurred. By day 3 of curing, the inner membranes of the mitochondria also appeared indistinct. Further, on day 5 of curing, the mitochondria exhibited swelling and rupture, with partial dissolution of the mitochondrial membranes. On day 7 of curing, mitochondrial swelling became more pronounced, the characteristic network structure had almost disappeared, and vacuole-like structures appeared internally. Compared to the control group, the $NaNO_2$ group maintained better mitochondrial integrity, with some intact mitochondria still visible on day 7 of curing. This indicates that low-dose sodium nitrite slowed the degree of mitochondrial rupture and better preserved mitochondrial integrity.

In addition to mitochondrial swelling and membrane permeability, the microstructure of mitochondria is also an important indicator of

Table 1
Effect of low-dose nitrite on the mitochondrial lipid oxidation products(mg/kg).

Lipid Oxidation Products	Control					Mean	Standard error	$NaNO_2$					Mean	Standard error	P value	VIP value
	0 h	1d	3d	5d	7d			0 h	1d	3d	5d	7d				
Aldehydes	89.39	91.37	58.98	191.69	144.31	–	–	89.39	53.28	142.12	169.42	118.51	–	–	–	–
5,9,13-trimethyl-4,8,12-Tetradecatrienal	8.55	20.22	20.72	19.39	12.71	15.94	0.72	8.55	2.47	10.41	19.47	12.98	10.68	0.82	<0.0001	0.66
Decanal	32.29	25.52	10.59	63.22	42.29	34.81	2.64	32.29	12.25	44.48	55.00	38.78	38.56	1.55	0.045	0.97
Hexadecanal	2.21	3.64	3.50	1.71	12.67	4.61	0.56	2.21	2.20	5.89	5.78	3.67	3.96	0.24	0.288	0.38
Lauryl aldehyde	3.45	4.24	4.10	3.35	2.78	3.53	0.10	3.45	1.83	3.11	3.35	2.80	2.86	0.10	<0.0001	0.23
Nonanal	38.41	23.56	10.01	70.48	56.22	39.57	3.08	38.41	12.62	48.19	54.30	41.05	38.91	2.09	0.860	1.06
Octanal	3.12	10.02	7.62	32.00	14.63	13.69	1.45	3.12	10.32	28.08	29.37	17.87	17.22	1.38	0.048	0.85
Undecanal	1.36	4.17	2.45	1.54	3.01	2.47	0.15	1.36	1.60	1.96	2.14	1.36	1.72	0.07	<0.0001	0.23
Alcohols	4.06	4.44	4.06	6.99	5.06	–	–	4.06	3.75	4.77	7.87	7.06	–	–	–	–
2-Ethylhexanol	1.24	1.25	1.18	1.11	0.65	1.08	0.05	1.24	2.83	1.15	2.23	4.10	2.25	0.17	<0.0001	0.32
1-Dodecanol	2.82	3.19	2.88	5.88	4.41	3.72	0.19	2.82	0.92	3.62	5.64	2.97	3.23	0.22	0.099	0.32
Acid	15.48	3.54	2.82	5.84	3.98	–	–	15.48	2.36	2.87	5.07	2.39	–	–	–	–
Lauric acid	1.61	1.90	1.26	4.60	1.88	2.27	0.18	1.61	0.86	1.69	2.09	1.06	1.52	0.08	<0.01	0.29
Palmitic acid	13.87	1.64	1.57	1.24	2.10	3.98	0.69	13.87	1.50	1.19	2.99	1.33	4.11	0.69	0.893	0.39
Ester	10.49	15.40	11.77	15.18	10.77	–	–	10.49	10.97	13.28	24.77	20.64	–	–	–	–
Isopropyl myristate	4.62	6.13	5.07	6.34	4.41	5.39	0.15	4.62	2.69	4.68	14.68	10.65	7.56	0.65	0.002	0.50
2,2,4-Trimethyl-1,3-pentanediol diisobutyrate	2.29	1.67	1.41	2.68	1.27	1.88	0.09	2.29	2.22	2.13	1.57	1.35	1.85	0.07	0.765	0.16
Ethyl caprylate	2.01	5.06	4.12	3.62	3.35	3.61	0.17	2.01	4.86	3.93	6.42	7.38	4.92	0.27	<0.01	0.36
Isopropyl palmitate	0.88	1.75	0.87	1.53	1.27	1.26	0.06	0.88	0.71	1.53	1.35	1.11	1.14	0.05	0.118	0.13
Methyl palmitate	0.70	0.78	0.31	1.02	0.47	0.65	0.04	0.70	0.50	1.00	0.76	0.14	0.63	0.05	0.776	0.12
Ketones	13.45	26.06	26.70	25.94	20.48	–	–	13.45	27.56	25.20	28.78	7.27	–	–	–	–
6-Methylhept-5-en-2-one	3.84	12.97	9.23	15.71	9.22	10.12	0.60	3.84	15.74	17.27	18.74	5.00	12.08	0.94	0.083	0.38
Geranylacetone	9.60	13.09	17.47	10.23	11.27	12.31	0.41	9.60	11.82	7.93	10.04	2.27	8.20	0.47	<0.0001	0.52
Phenols	34.44	13.03	11.55	15.49	10.25	–	–	34.44	24.94	14.41	12.68	8.07	–	–	–	–
2,4-Di-tert-butylphenol	34.44	13.03	11.55	15.49	10.25	17.13	1.30	34.44	24.94	14.41	12.68	8.07	19.00	1.39	0.330	0.73
hydrocarbons	7.41	17.16	29.99	36.03	31.01	–	–	7.41	42.13	33.35	35.63	19.00	–	–	–	–
Cyclododecane	0.65	1.48	1.25	1.25	0.76	1.12	0.06	0.65	0.31	1.17	6.62	0.46	1.80	0.34	0.049	0.27
Hexadecane	3.01	5.44	9.13	2.69	2.67	4.60	0.36	3.01	3.34	4.14	8.38	3.07	4.41	0.29	0.679	0.20
Styrene	3.75	10.23	19.61	32.09	27.58	18.64	1.47	3.75	38.47	28.04	20.63	15.47	21.31	1.67	0.061	0.68

VIP value was obtained by OPLS-DA.

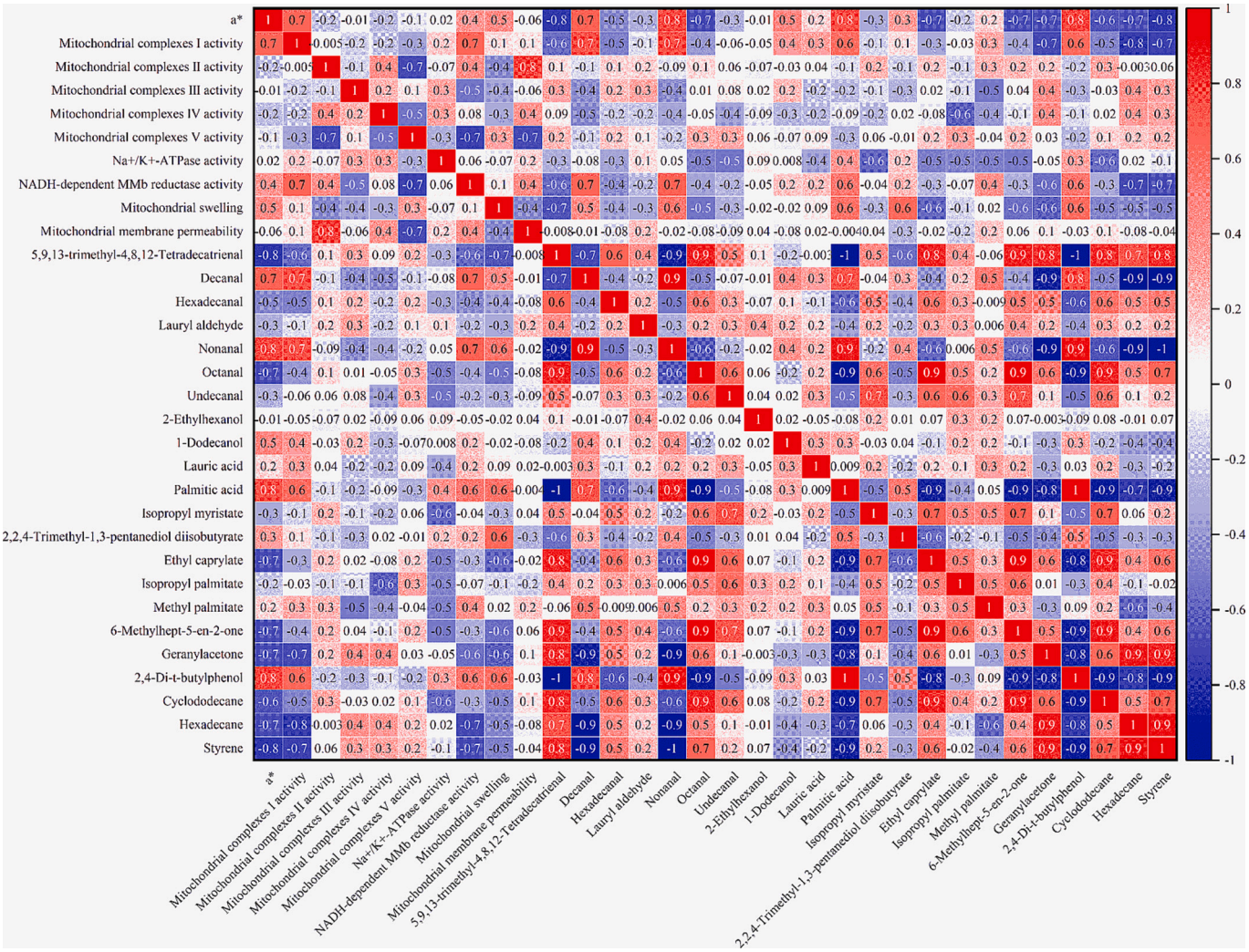

Fig. 4. Correlation analysis.

mitochondrial damage (Gao et al., 2013). In this study, the changes in mitochondrial microstructure were evident during the postmortem wet curing. Consistently, Zhu et al. (2023) observed the vacuolization of a mitochondrion with the disappearance of cristae at 5 d in postmortem yak muscle. Wang et al. (2021) found that most of the mitochondria disappeared at 7 d in postmortem yak muscle. Notably, the present study also suggests that low-dose sodium nitrite can better preserve mitochondrial integrity, which was supported by the results of mitochondrial swelling and mitochondrial membrane permeability, as discussed above. In addition, previous study has found a relationship between the generation of ROS and damage in mitochondrial microstructures, resulting in increased mitochondrial membrane permeability (Zou, Shao, et al., 2023). Accordingly, it is speculated that low-dose sodium nitrite maintains mitochondrial structural integrity by inhibiting the production of ROS by mitochondria (Raat et al., 2009).

3.4. Changes in mitochondrial lipid oxidation products

In addition to the morphology perspective, this study also investigated changes in the mitochondrial lipid bilayer from the perspective of lipid oxidation to illustrate the extent of mitochondrial damage in yak meat during the wet curing. SPME-GC–MS technology was employed to analyze the changes in volatile mitochondrial lipid oxidation products in control and $NaNO_2$ groups of yak meat at 0, 1, 3, 5, and 7 days of curing. The total ion chromatograms of volatile compounds obtained via SPME-GC–MS are shown in Fig. S1. Compounds were identified through database searches and comparisons, focusing on aldehydes, alcohols, acids, and other lipid oxidation-related compounds. The results are presented in Table 1.

Table 1 shows that with the extension of curing time, lipid oxidation occurred in both the control and $NaNO_2$ the mitochondria of both the control and $NaNO_2$ groups. A total of 22 different lipid oxidation products, including aldehydes, alcohols, and esters, were detected, with 7 aldehydes and 5 esters accounting for 55 % of the compound types. Compounds such as 5,9,13-trimethyl-4,8,12-tetradecatrienal, decanal, lauryl aldehyde, octanal, undecanal, 2-ethylhexanol, lauric acid, isopropyl myristate, ethyl caprylate, geranylacetone, and cyclododecane showed significant differences between the control and $NaNO_2$ groups. As the curing time extended, the $NaNO_2$ group showed a reduction in the generation of lipid oxidation products to varying degrees, indicating that low-dose sodium nitrite slowed the process of mitochondrial lipid oxidation, reduced mitochondrial damage, and contributed positively to maintaining mitochondrial integrity.

Lipid oxidation is generally initiated by free radicals produced during respiration. Initially, these free radicals break the non-conjugated double bonds of unsaturated fatty acids to form conjugated double bonds. Subsequently, these conjugated double bonds break to form hydroperoxides, which is the main reaction in the early stages of lipid oxidation. Hydroperoxides are unstable and gradually decompose into stable secondary metabolites, the most typical of which are aldehyde

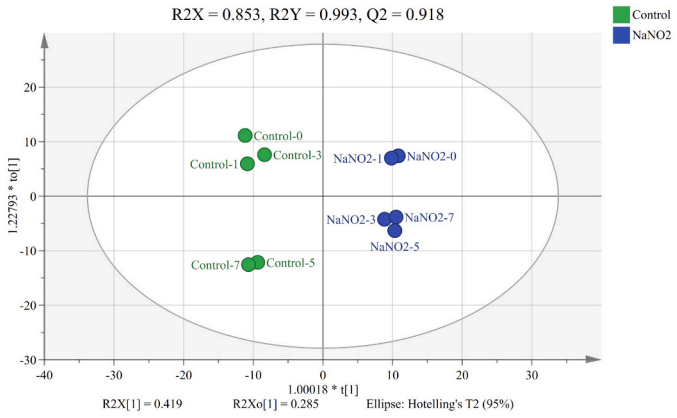

(A)

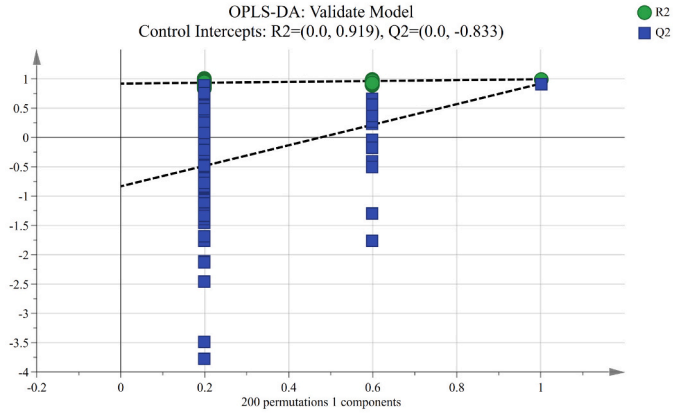

(B)

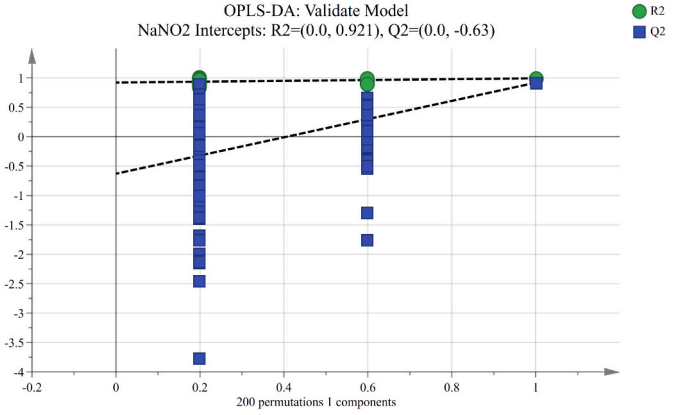

(C)

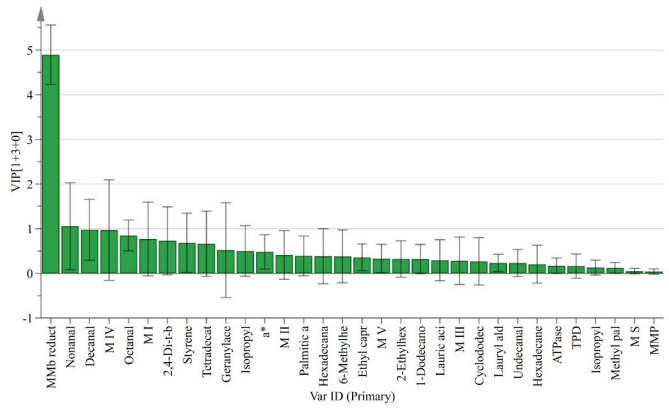

(D)

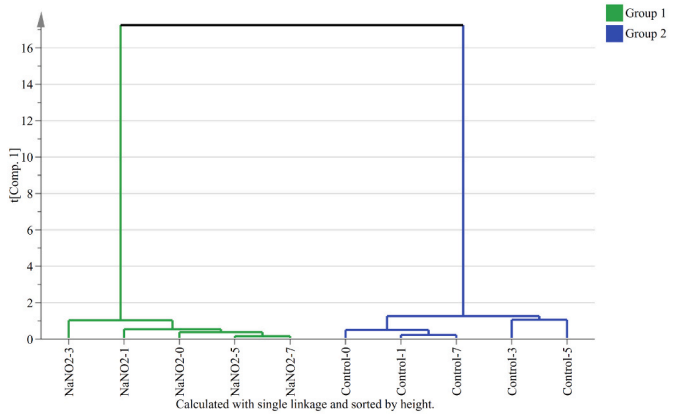

(E)

Fig. 5. Orthogonal Partial Least Squares Discriminant Analysis. (A) Score Scatter Plot. (B) Validate Model for Control Group. (C) Validate Model for $NaNO_2$ Group. (D) Variable Importance in Projection, (VIP). M I: Mitochondrial complexes I activity. M II: Mitochondrial complexes II activity. M III: Mitochondrial complexes III activity. M IV: Mitochondrial complexes IV activity. M V: Mitochondrial complexes V activity. ATPase: Na^+/K^+-ATPase activity. MMb reductase: NADH-dependent MMb reductase activity. M S: Mitochondrial swelling. MMP: Mitochondrial membrane permeability. Tetradecatrienal: 5,9,13-trimethyl-4,8,12-Tetradecatrienal. TPD: 2,2,4-Trimethyl-1,3-pentanediol diisobutyrate. (E) Hierarchical Clustering.

compounds. The formation of substantial secondary lipid oxidation products indicates that the lipid oxidation reaction has entered a late stage (Faustman et al., 2010). Early studies by Yin and Faustman (1993) demonstrated that lipid oxidation accelerated the oxidation of horse heart oxymyoglobin during in vitro incubation with myoglobin. This finding suggests that oxidation products derived from unsaturated fatty acids in liposomes interact with myoglobin. Studies by Lynch and Faustman (2000) found that the lipid oxidation product 4-hydroxy-2-nonenal promoted myoglobin oxidation and inhibited the reduction of metmyoglobin, suggesting that aldehyde lipid oxidation products can covalently modify myoglobin and metmyoglobin reductase, thus affecting protein stability. Numerous studies have demonstrated that lipid oxidation is directly related to meat color deterioration and oxidative rancidity (Alicia et al., 2011; Faustman et al., 2010; Kim et al., 2013). In this study, a significant number of lipid oxidation products, primarily decanal, nonanal, and octanal, were produced during mitochondrial lipid oxidation. Further research is needed to determine whether these products are related to changes in the a^* value of yak meat.

3.5. Correlation analysis

To determine the relationship between the a^* value and mitochondrial-related enzyme activities, swelling and membrane permeability, and lipid oxidation products, a correlation analysis was conducted, and the results are shown in Fig. 4. The study revealed that the activity of mitochondrial complexes I and mitochondrial swelling, two indicators of mitochondrial functional structure, were significantly positively correlated with a^*. NADH-dependent metmyoglobin reductase activity also showed a significant positive correlation with a^*. Among the lipid oxidation products, decanal, nonanal, 1-dodecanol, palmitic acid, and 2,4-Di-tert-butylphenol were significantly positively correlated with a^*, while 2,2,4-trimethyl-1,3-pentanediol diisobutyrate and methyl palmitate were positively correlated with a^*. Conversely, nine lipid oxidation products, including 5,9,13-trimethyl-4,8,12-tetradecatrienal, hexadecanal, octanal, ethyl caprylate, 6-methylhept-5-en-2-one, geranylacetone, cyclododecane, hexadecane, and styrene, were significantly negatively correlated with a^*, and lauryl aldehyde, undecanal, isopropyl myristate, and isopropyl palmitate were negatively correlated with a^*. This correlation analysis revealed a strong relationship between the changes in mitochondrial functional characteristics and microstructure in yak meat during the wet curing and the a^* value, suggesting that mitochondrial status significantly influences meat color during curing. The positive correlations with specific lipid oxidation products suggest that these compounds may play a role in maintaining meat redness. In contrast, the negative correlations with other oxidation products indicate that they may contribute to meat discoloration.

3.6. Orthogonal partial least squares discriminant analysis

To further identify the significant indicators and factors influencing the a^* value changes in yak meat during the wet curing with low-dose sodium nitrite, OPLS-DA analysis was performed, and the results are shown in Fig. 5. As seen in Fig. 5 (A), the R^2X (coefficient of determination for the explanatory variables) is 0.853, the R^2Y (coefficient of determination for the response variables) is 0.993, and the Q^2 (predictive capability of the model) is 0.918, indicating a 91.8 % prediction rate for the two groups of variables. The control group and the $NaNO_2$ group are distinguished on the horizontal axis of the Score Scatter Plot, with the control group variables distributed on the negative half-axis and the $NaNO_2$ group variables on the positive half-axis, indicating a clear distinction between the variables of the two groups. Additionally, the model was cross-validated (Figs. 5 (B) and (C)), with R^2 values of 0.919 and 0.921 and absolute Q^2 values of 0.833 and 0.63 for the control and $NaNO_2$ groups, respectively, both greater than 0.5, indicating that the model fitting results are acceptable (Yun et al., 2021). The Hierarchical Clustering results (Fig. 5 (E)) showed that the control group and the $NaNO_2$ group can be divided into two categories, further validating the distinction shown in the Score Scatter Plot.

According to the Variable Importance in Projection (VIP, Fig. 5 (D) and Table 1), combined with the P values of the lipid oxidation products in Table 1 and the correlation analysis results, significant indicators of a^* changes influenced by low-dose sodium nitrite were identified. These indicators had an absolute correlation coefficient with a^* greater than 0.4, $P < 0.05$, and VIP > 0.5. The results show that low-dose sodium nitrite significantly influences two mitochondrial function indicators: mitochondrial complexes I activity and NADH-dependent metmyoglobin reductase activity. Additionally, three aldehyde products (5,9,13-trimethyl-4,8,12-tetradecatrienal, decanal and octanal) and one ketone product (geranylacetone) among the mitochondrial lipid oxidation products contribute significantly to the changes in a^*. Therefore, mitochondrial complexes I activity and NADH-dependent metmyoglobin reductase activity are the main indicators influencing the changes in a^*, while 5,9,13-trimethyl-4,8,12-tetradecatrienal, decanal, octanal, and geranylacetone are the main factors influencing the changes in a^*.

4. Conclusion

This research provided a detailed understanding of how low-dose sodium nitrite influences yak meat color and mitochondrial function during the wet curing. Low-dose sodium nitrite improved the redness of yak meat by enhancing mitochondrial complex activities and protecting mitochondrial structure. Sodium nitrite reduced mitochondrial swelling and membrane permeability, thereby preserving mitochondrial function. Key factors influencing meat color included mitochondrial complex I activity, NADH-dependent metmyoglobin reductase activity, and four lipid oxidation products: 5,9,13-trimethyl-4,8,12-tetradecatrienal, decanal, octanal, and geranylacetone. Future research could further explore the specific mechanisms of these factors in meat color changes, providing valuable insights into the quality of cured meat products.

Informed consent

Informed consent was obtained from all individual participants included in the study.

CRediT authorship contribution statement

Zhuo Wang: Writing – original draft, Investigation, Formal analysis, Data curation. **Jibing Ma:** Writing – review & editing, Formal analysis, Data curation. **Guoyuan Ma:** Writing – review & editing, Funding acquisition. **Qunli Yu:** Supervision. **Ling Han:** Supervision. **Li Zhang:** Supervision.

Declaration of competing interest

No conflict of interest exits in the submission of this manuscript, and manuscript is approved by all authors for publication. I would like to declare on behalf of my co-authors that the work described was original research that has not been published previously, and not under consideration for publication elsewhere, in whole or in part. All the authors listed have approved the manuscript that is enclosed.

Data availability

The data that has been used is confidential.

Acknowledgements

This work was supported by the National Natural Science Foundation of China (32360556), the Scientific Research Start-up Funds of Gansu Agricultural University (GAU-KYQD-2021-19), the National Key

Research and Development of China (2021YFD1600204-2), the National Yak Technology Innovation Center (2023-NK-J07), and the program for Agriculture Research System of China (No. CARS-37).

Appendix A. Supplementary data

Supplementary data to this article can be found online at https://doi.org/10.1016/j.fochx.2024.102095.

References

Alazoumi, K. K. M., Ahmed, A., Alamery, S. F., Shamsi, A., Ahmad, B., Islam, A., et al. (2021). Effect of antioxidants on heavy metals induced conformational alteration of cytochrome c and myoglobin. *Protein and Peptide Letters, 28*, 31–42.

Alicia, O., Kseniya, D., José Luis, N., David, S., Patrik, S. L., & Mónica, F. (2011). SPME -GC-MS versus selected ion flow tube mass spectrometry (SIFT-MS) analyses for the study of volatile compound generation and oxidation status during dry fermented sausage processing. *Journal of Agricultural and Food Chemistry, 59*(5), 1931–1938.

Angelo, D. A., Cristina, M., Sara, R., Cristiana, M., Sebastiana, F., & Lello, Z. (2012). Chianina beef tenderness investigated through integrated omics. *Journal of Proteomics, 75*, 4381–4398.

Attri, P., Jha, I., Choi, E. H., & Venkatesu, P. (2014). Variation in the structural changes of myoglobin in the presence of several protic ionic liquid. *International Journal of Biological Macromolecules, 69*, 114–123.

Bedale, W., Sindelar, J. J., & Milkowski, A. L. (2016). Dietary nitrate and nitrite: Benefits, risks, and evolving perceptions. *Meat Science, 120*, 85–92.

Bekhit, A., Geesink, G., Morton, J., & Bickerstaffe, R. (2001). Metmyoglobin reducing activity and colour stability of ovine *longissimus* muscle. *Meat Science, 57*, 427–435.

Belskie, K. M., Buiten, C. B. V., Ramanathan, R., & Mancini, R. A. (2015). Reverse electron transport effects on NADH formation and metmyoglobin reduction. *Meat Science, 105*, 89–92.

Boyman, L., Karbowski, M., & Lederer, W. J. (2020). Regulation of mitochondrial ATP production: Ca^{2+} signaling and quality control. *Trends in Molecular Medicine, 26*, 21–39.

Bueno, M., Resconi, V. C., Campo, M. M., Ferreira, V., & Escudero, A. (2019). Development of a robust HS-SPME-GC-MS method for the analysis of solid food samples. Analysis of volatile compounds in fresh raw beef of differing lipid oxidation degrees. *Food Chemistry, 281*, 49–56.

Chen, C., Yu, Q., Han, L., Zhang, J., & Guo, Z. (2018). Effects of aldehyde products of lipid oxidation on the color stability and metmyoglobin reducing ability of bovine *longissimus* muscle. *Animal Science Journal, 89*, 810–816.

Chkadua, G., Nozadze, E., Tsakadze, L., Shioshvili, L., Arutinova, N., Leladze, M., et al. (2022). Effect of H_2O_2 on Na, K-ATPase. *Journal of Bioenergetics and Biomembranes, 54*, 241–249.

Elroy, N. N., Rogers, J., Mafi, G. G., VanOverbeke, D. L., Hartson, S. D., & Ramanathan, R. (2015). Species-specific effects on non-enzymatic metmyoglobin reduction in vitro. *Meat Science, 105*, 108–113.

Faustman, C., Sun, Q., Richard Mancini, R., & Suman, S. P. (2010). Myoglobin and lipid oxidation interactions: Mechanistic bases and control. *Meat Science, 86*, 86–94.

Gagaoua, M., Terlouw, E. M. C., Micol, D., Boudjellal, A., Hocquette, J. F., & Picard, B. (2015). Understanding early post-mortem biochemical processes underlying meat color and pH decline in the *longissimus thoracis* muscle of young blond d'aquitaine bulls using protein biomarkers. *Journal of Agricultural and Food Chemistry, 63*, 6799–6809.

Gao, X., Wang, Z., Tang, M., & Dai, R. (2014). Comparsion of the effects of succinate and NADH on postmortem metmyoglobin reductase activity and beef colour stability. *Journal of Integrative Agriculture, 13*, 1817–1826.

Gao, X., Xie, L., Wang, Z., Li, X., Luo, H., Ma, C., et al. (2013). Effect of postmortem time on the metmyoglobin reductase activity, oxygen consumption, and colour stability of different lamb muscles. *European Food Research and Technology, 236*, 579–587.

Genova, M. L., & Lenaz, G. (2013). Functional role of mitochondrial respiratory supercomplexes. *Biochimica et Biophysica Acta, 1837*, 427–443.

Griffiths, E. J. (2000). Mitochondria-potential role in cell life and death. *Cardiovascular Research, 46*, 24–27.

Gupta, J., Bower, C. G., Sullivan, G., & Cavender, G. (2018). Effect of differing ingredients and packaging technologies on the color of high-pressure processed ground beef. *Journal of Food Quality, 2018*, 1–5.

Kamga, C., Krishnamurthy, S., & Shiva, S. (2012). Myoglobin and mitochondria: A relationship bound by oxygen and nitric oxide. *Nitric Oxide, 26*(4), 251–258.

Kim, H. W., Choi, Y. S., Choi, J. H., Kim, H. Y., Hwang, K. E., Song, D. H., et al. (2013). Antioxidant effects of soy sauce on color stability and lipid oxidation of raw beef patties during cold storage. *Meat Science, 95*(3), 641–646.

Kuleva, N. V., Krasovskaya, I., & E.. (2016). A new role for myoglobin in cardiac and skeletal muscle function. *Biophysics, 61*, 717–720.

Lee, S., Lee, H., Kim, S., et al. (2018). Microbiological safety of processed meat products formulated with low nitrite concentration: A Mini review. *Asian-Australasian Journal of Animal Sciences, 31*(8), 1073–1077.

Li, H., Samouilov, A., Liu, X., & Zweier, J. L. (2004). Characterization of the effects of oxygen on xanthine oxidase-mediated nitric oxide formation. *Journal of Biological Chemistry, 279*, 16939–16946.

Li, M., Li, X., Xin, J., Li, Z., Li, G., Zhang, Y., et al. (2017). Effects of protein phosphorylation on color stability of ground meat. *Food Chemistry, 219*, 304–310.

Lynch, M. P., & Faustman, C. (2000). Effect of aldehyde lipid oxidation products on myoglobin. *Journal of Agricultural and Food Chemistry, 48*(48), 600–604.

Ma, G., Chen, H., Zhang, Q., Ma, J., Yu, Q., Han, L., et al. (2019). Protective characterization of low dose sodium nitrite on yak meat myoglobin in a hydroxy radical oxidation environment: Fourier transform infrared spectroscopy and laser Micro-Raman spectroscopy. LWT–food. *Science and Technology, 116*, Article 108556.

Ma, G., Wang, Z., Chen, H., Yu, Q., & Han, L. (2021). Effect of low-dose sodium nitrite treatment on the endogenous antioxidant capacity of yak meat during wet curing: Pros and cons. LWT–food. *Science and Technology, 141*, Article 110879.

Ma, G., Wang, Z., Yu, Q., Han, L., Chen, C., & Guo, Z. (2022). Effects of low-dose sodium nitrite on the structure of yak meat myoglobin during wet curing. *Food Chemistry: X, 15*, Article 100434.

Mancini, R. A., & Hunt, M. C. (2005). Current research in meat color. *Meat Science, 71*, 100–121.

Mancini, R. A., & Ramanathan, R. (2014). Effects of postmortem storage time on color and mitochondria in beef. *Meat Science, 98*, 65–70.

Raat, N. J. H., Shiva, S., & Gladwin, M. T. (2009). Effects of nitrite on modulating ROS generation following ischemia and reperfusion. *Advanced Drug Delivery Reviews, 61*, 339–350.

Ramanathan, R., Mancini, R., Joseph, P., & Suman, S. (2013). Bovine mitochondrial oxygen consumption effects on oxymyoglobin in the presence of lactate as a substrate for respiration. *Meat Science, 93*, 893–897.

Reddy, I., & M., & Carpenter, C. E.. (1991). Determination of metmyoglobin reductase activity in bovine skeletal muscles. *Journal of Food Science, 1991*(56), 1161–1164.

Rybka, V., Suzuki, Y. J., Gavrish, A. S., Dibrova, V. A., Gychka, S. G., & Shults, N. V. (2019). Transmission electron microscopy study of mitochondria in aging brain synapses. *Antioxidants, 8*, 171.

Sallan, S., Kaban, G., Oğraş, Ş.Ş., Murat Çelik, M., & Kaya, M. (2020). Nitrosamine formation in a semi-dry fermented sausage: Effects of nitrite, ascorbate and starter culture and role of cooking. *Meat Science, 159*, Article 107917.

Sullivan, G. A., & Sebranek, J. G. (2012). Nitrosylation of myoglobin and nitrosation of cysteine by nitrite in a model system simulating meat curing. *Journal of Agricultural and Food Chemistry, 60*, 1748–1754.

Suman, S. P., & Joseph, P. (2013). Myoglobin chemistry and meat color. *Annual Review of Food Science and Technology, 4*, 79–99.

Tang, J., Faustman, C., Hoagland, T. A., Mancini, R. A., & Hunt, M. C. (2005). Postmortem oxygen consumption by mitochondria and its effects on myoglobin form and stability. *Journal of Agricultural and Food Chemistry, 53*, 1223–1230.

Tang, J., Faustman, C., Mancini, R. A., Mark, S., & Hunt, M. C. (2005). Mitochondrial reduction of metmyoglobin: Dependence on the electron transport chain. *Journal of Agricultural and Food Chemistry, 53*, 5449–5455.

Tuell, J. R., Kim, H. W., Zhang, J., Guedes, J., Seo, J. K., Schoonmaker, J. P., et al. (2021). Arginine supplementation may improve color and redox stability of beef loins through delayed onset of mitochondrial-mediated apoptotic processes. *Food Chemistry, 343*, Article 128552.

Wang, L., Du, R., Li, J., Cai, Z., Han, L., Mao, Y., et al. (2021). The potential mediation of nitric oxide in the activation of mitochondrion-dependent apoptosis and yak meat tenderness during postmortem aging. *Food Bioscience, 42*, Article 101131.

Wang, L., Ma, G., Zhang, Y., Shi, X., Han, L., Yu, Q., et al. (2018). Effect of mitochondrial cytochrome c release and its redox state on the mitochondrial-dependent apoptotic cascade reaction and tenderization of yak meat during postmortem aging. *Food Research International, 111*, 488–497.

Washington, T. A., Reecy, J. M., Thompson, R. W., Lowe, L. L., Mcclung, J. M., & Carson, J. A. (2008). Lactate dehydrogenase expression at the onset of altered loading in rat soleus muscle. *Journal of Applied Physiology, 97*, 1424–1430.

Wink, D. A., Miranda, K. M., Espey, M. G., Pluta, R. M., Hewett, S. J., Colton, C., et al. (2001). Mechanisms of the antioxidant effects of nitric oxide. *Antioxidants & Redox Signaling, 3*, 203–213.

Yin, M. C., & Faustman, C. (1993). Influence of temperature, pH, and phospholipid composition upon the stability of myoglobin and phospholipid: Liposome model. *Journal of Agricultural and Food Chemistry, 41*(6), 853–857.

Yun, J., Cui, C., Zhang, S., Zhu, J., Peng, C., Cai, H., & Hou, R. (2021). Use of headspace GC/MS combined with chemometric analysis to identify the geographic origins of black tea. *Food Chemistry, 360*, Article 130033.

Zhang, J., Li, M., Yu, Q., Han, L., & Ma, Z. (2019). Effects of lysosomal-mitochondrial apoptotic pathway on tenderness in post-mortem bovine *longissimus* muscle. *Journal of Agricultural and Food Chemistry, 67*, 4578–4587.

Zhang, J., Yu, Q., Han, L., Chen, C., Li, H., & Han, G. (2017). Study on the apoptosis mediated by cytochrome c and factors that affect the activation of bovine *longissimus* muscle during postmortem aging. *Apoptosis, 22*, 777–785.

Zhang, J., Yu, Q., Han, L., Han, M., & Han, G. (2020). Effects of lysosomal iron involvement in the mechanism of mitochondrial apoptosis on postmortem muscle protein degradation. *Food Chemistry, 328*, Article 127174.

Zhao, R. Z., Jiang, S., Zhang, L., & Yu, Z. B. (2019). Mitochondrial electron transport chain, ROS generation and uncoupling. *International Journal of Molecular Medicine, 42*, 3–15.

Zhu, X., Dingkao, R., Sun, N., Han, L., & Yu, Q. (2023). The potential mediation of hypoxia-inducible factor-1α in heat shock protein 27 translocations, caspase-3 and calpain activities and yak meat tenderness during postmortem aging. *Meat Science, 204*, Article 109264.

Zou, B., Jia, F., Ji, L., et al. (2023). Effects of mitochondria on postmortem meat quality: Characteristic, isolation, energy metabolism, apoptosis and oxygen consumption. *Critical Reviews in Food Science and Nutrition, 64*(30), 11239–11262.

Zou, B., Shao, L., Yu, Q., Zhao, Y., Li, X., & Dai, R. (2023). Changes of mitochondrial lipid molecules, structure, cytochrome c and ROS of beef *longissimus lumborum* and *psoas*

major during postmortem storage and their potential associations with beef quality. *Meat Science, 195*, Article 109013.